

Inhibitory Effect Against Akt by Cyclic Dipeptides Isolated from *Bacillus* sp.

Hong, Sungwon¹, Byoung-Ho Moon¹, Yeonjoong Yong¹, Soon Young Shin², Young Han Lee², and Yoongho Lim^{1*}

¹Bio/Molecular Informatics Center, Division of Bioscience and Biotechnology, Konkuk University, Seoul 143-701, Korea

²Institute of Biomedical Science and Technology, Konkuk University, Seoul 143-701, Korea

Received: October 2, 2007 / Accepted: December 1, 2007

Among thirteen strains of the genus *Bacillus* isolated from Shrimp-jeotkal in our laboratory, a strain BA34 showing good antifungal activity against *Phytophthora infestans* in a previous experiment was tested for the inhibitory effect against Akt, protein kinase B. Since Akt is known to play an important role in controlling apoptosis, its inhibitors can be used as potential apoptosis-inducing agents in the treatment of cancer. Two active compounds were isolated and their structures were determined. They have similar structures, despite showing different inhibitory effects. In order to elucidate the reasons for these different effects, three-dimensional studies were carried out.

Keywords: *Bacillus* sp., cyclic dipeptide, Akt

The serine/threonine kinase Akt, also known as protein kinase B, plays an important role in regulating cellular growth and apoptosis [8]. Upon growth factor stimulation, Akt is activated by phosphorylation at two residues, Ser-473 and Thr-308, via the phosphatidylinositol 3-kinase (PI-3K) pathway [1]. Constitutive activation of Akt has been detected in a wide variety of human malignancies [2]. Furthermore, exogenous expression of Akt inhibits apoptosis and induces malignant transformation, whereas inhibition of Akt stimulates apoptosis [11]. These observations implicate the Akt as an attractive target for cancer therapy.

In order to discover natural products showing the inhibitory effect against Akt, the fermented broths of microorganisms were tested. Thirteen strains of the genus *Bacillus* were isolated from Shrimp-jeotkal in our laboratory. Among them, a strain BA34 showed good antifungal activity against *Phytophthora infestans* in the previous experiments [4]. Based on its partial sequence of 16S rDNA and its image obtained from scanning electron microscopy, it was identified as a *Bacillus* strain with 99%

homology to *Bacillus amyloliquefaciens*. In this experiment, the fermented broth of BA34 was tested for Akt inhibition.

BA34 was grown in a 500-ml Erlenmeyer flask with Tryptic Soy Broth (TSB, 7 g) on a rotary shaker at 160 rpm and at 37°C for 3 days. Two hundred ml of the culture medium was mixed with the same amounts of methanol (MeOH). The mixture was shaken for 12 h and then was filtered through a 0.45 µm filter unit to get rid of the BA34. The filtrate was concentrated *in vacuo* and dissolved in 100 ml of acetonitrile (AcCN). The shaking flask culture was centrifuged at 8,000 rpm for 10 min. The supernatant was concentrated *in vacuo* using a rotary evaporator, and then applied to Prep-HPLC (Varian, Walnut Creek, CA, U.S.A.) using a C₁₈ Phenomenex Gemini column (250 mm × 10.00 mm, 5 µm, Phenomenex, Torrance, CA, U.S.A.) with H₂O/AcCN (80:20) to yield fractions (F1 to F6). Of these, the fraction 2 (F2) showing Akt inhibitory effect was collected and considered to be a single compound based on the chromatogram of the photodiode array detector. Another fraction showing an inhibitory effect, the fraction 1 (F1), was not a single compound, and thus it was separated using Prep-HPLC on a C₁₈ Phenomenex Gemini column with H₂O/AcCN (85:15) to yield fractions (F1-1 to F1-4). The fraction F1-4 showing Akt inhibitory effect was collected and confirmed to be a single compound based on the chromatogram of the photodiode array detector [5]. The procedure to isolate F2 and F1-4 is shown in Fig. 1.

Akt activation is mainly induced by the phosphorylation of residue Ser-473 or Thr-308. In order to investigate whether F2 and F1-4 affect the activation of Akt, the phosphorylation status of Akt was measured using Western blot analysis with a phospho-specific antibody against the Ser-473 residue. U-87MG cells (1.5 × 10⁶ cells) were seeded onto 60-mm plates. After 24 h, U-87MG cells were serum-starved with 0.5% fetal bovine serum (FBS) for 24 h, followed by treatment with F2 or F1-4 at a concentration of 10 µg/ml. After 30 min, U-87MG cells were harvested and lysed in the buffer solution (1% Triton X-100, 0.15 M NaCl, 50 mM Tris-HCl, 1 mM EDTA, 10% glycerol) for

*Corresponding author

Phone: 82-2-450-3760; Fax: 82-2-456-3761;
E-mail: yoongho@konkuk.ac.kr

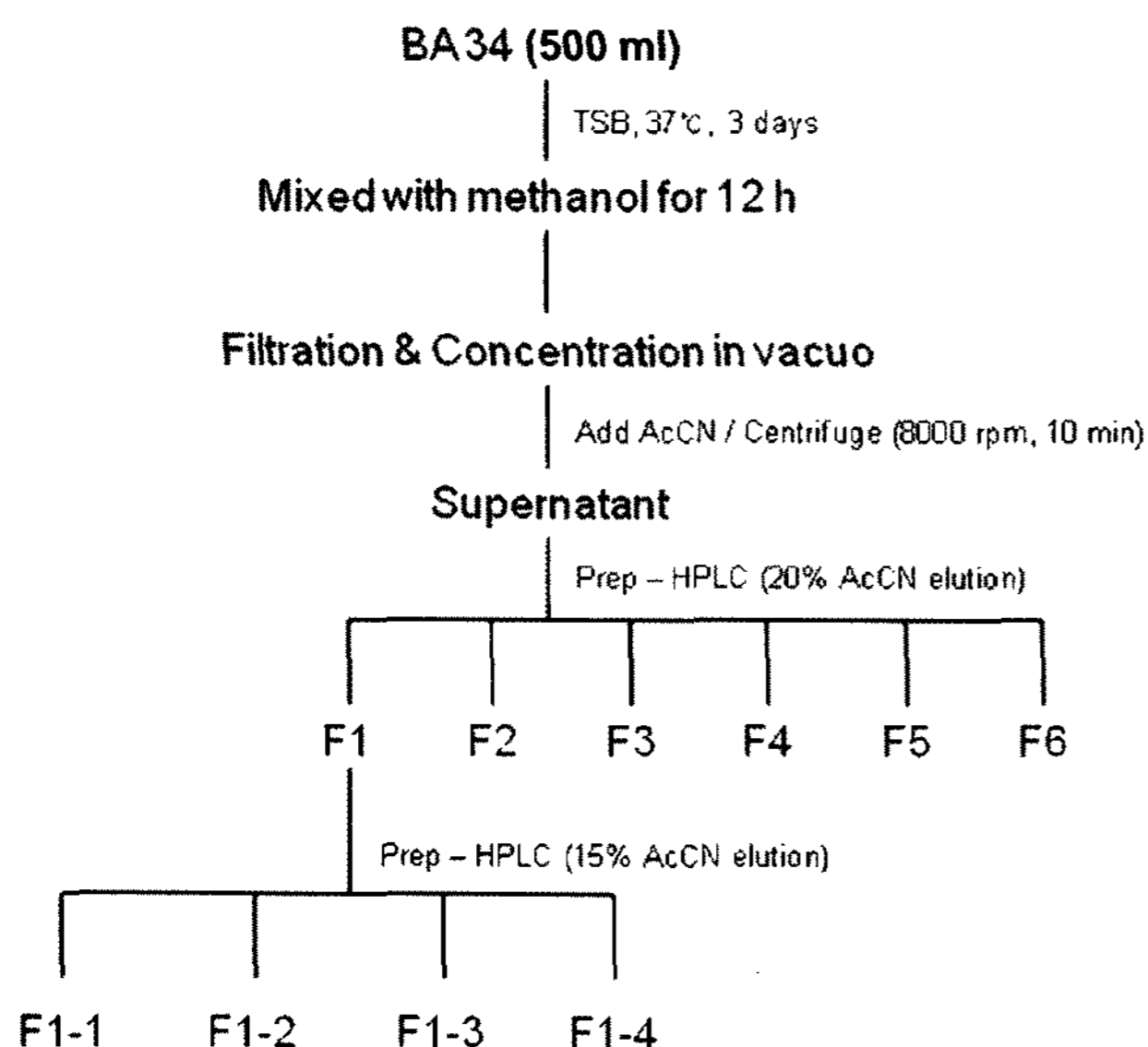


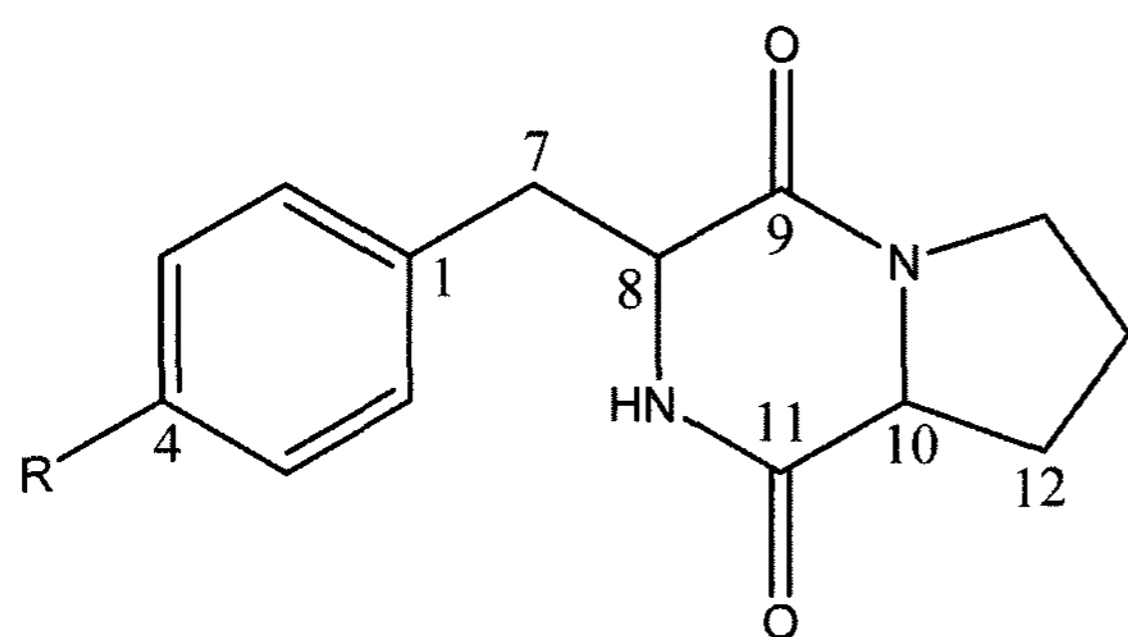
Fig. 1. Scheme for isolation of F2 and F1-4 (TSB, Tryptic Soy Broth; AcCN, acetonitrile).

30 min at 4°C. The lysate was centrifuged at 15,000 $\times g$ for 15 min to separate the extracted proteins from cell debris. Protein concentration was measured using the bicinchoninic acid (BCA) protein assay reagent (Pierce Biotechnology Inc., Rockford, IL, U.S.A.). Fifteen μg of protein was separated by 8% SDS-polyacrylamide gel electrophoresis and transferred to nitrocellulose membrane. For Western blot analysis, the membrane was blocked with 5% skim milk for 30 min, and then incubated with the rabbit anti-phospho-Akt (ser473) antibody (Cell Signaling Technology, Danvers, MA, U.S.A.) or mouse anti-glyceraldehydes-3-phosphate dehydrogenase (GAPDH) antibody (Santa Cruz Biotechnology, CA, U.S.A.) as an internal control for protein contents. After the incubation of primary antibody, the membrane was washed three times with Tween-20 Tris-buffer saline (TTBS) buffer (25 mM Tris-HCl, pH 7.5, 150 mM NaCl, 0.05% Tween-20), and then incubated with horseradish peroxidase-conjugated secondary antibody for 90 min. After washing the membrane three times with TTBS buffer, the blots were developed by using an enhanced chemiluminescence detection system (Amersham Pharmacia Biotech, Piscataway, NJ, U.S.A.). The relative band intensities were measured by a quantitative scanning densitometer and image analysis software, Bio-1D version 97.04. Values are plotted as mean \pm SD ($n=3$). The statistical significance of the assay was evaluated using Student's *t*-test.

The structures of the isolated compounds (F2 and F1-4) were identified using nuclear magnetic resonance (NMR) spectroscopy. All NMR experiments were performed using a Bruker Avance 400 spectrometer system (Bruker, Karlsruhe, Germany) [6]. The 1H NMR spectrum of F2 in MeOH- d_4 revealed eight signals, two of which displayed

aromatic signals at 6.63 and 7.04 ppm. Six showed aliphatic signals from 1.71 to 4.24 ppm. The ^{13}C and distortionless enhancement by polarization transfer (DEPT) NMR spectra showed the presence of twelve carbons, including two carbonyl signals at 165.1 and 168.9 ppm, four aromatic signals ranging from 114.7 to 155.9 ppm, two methine signals at 56.0 and 58.4 ppm, and four methylene signals from 21.8 to 44.5 ppm. Two doublets at 7.04 and 6.63 ppm ($J=8.5$ Hz) in the 1H NMR spectrum of F2 showed a set of AB signals in the aromatic ring because the integration indicated four protons in this AB system. In order to clarify the result obtained from the interpretation of NMR data, mass spectrometry was carried out on a JMS-700 Mstation (JEOL Ltd., Japan). The mass spectrum of F2 supported a molecular formula of $C_{14}H_{16}N_2O_3$, which gave a molecular ion peak at m/z 260, in agreement with both the 1H and ^{13}C NMR spectra described above. The direct connections between 1H signals and ^{13}C signals were determined by the heteronuclear multiple quantum coherence (HMQC) experiments. The correlated spectroscopy (COSY) experiment supported a coupling relationship between aliphatic protons as two parts. Two 1H peaks at 4.24 and 2.92 ppm were correlated with each other and four 1H peaks at 4.04, 1.40, 1.71, and 3.33 ppm were also correlated with each other. The connectivity among these partial structures was determined by the heteronuclear multiple bonded connectivities (HMBC) spectroscopic data. In the HMBC spectrum, the 1H peak at 4.24 ppm, was an long-range coupled to the ^{13}C peak at 127.0 ppm which was aromatic quaternary carbon, and 165.1 ppm, which was a carbonyl carbon. Therefore, aromatic ring was connected to one of the aliphatic proton parts. The ^{13}C peak at 168.9 ppm, which was another carbonyl carbon, showed long-range coupling with the 1H peak at 4.04 ppm, which was the other aliphatic proton part from the HMBC spectrum. The 1H NMR spectrum of F2 in DMSO- d_6 showed two more protons, which were exchangeable, at 7.84 and 9.23 ppm. One of the exchangeable protons at 7.84 ppm was long-range coupled to the ^{13}C peak at 165.1 ppm, which was a carbonyl carbon, and 58.4 ppm, which was a methine carbon from the HMBC spectrum. Therefore, this exchangeable proton was connected to nitrogen, and the other exchangeable proton peak at 9.23 ppm should be hydroxide in the *para*-position of the aromatic ring. These assignments established the structure of F2 as cyclo(prolyltyrosyl) (Fig. 2). The complete assignments of the 1H and ^{13}C chemical shifts of cyclo(prolyltyrosyl) are listed in Table 1.

The ^{13}C NMR spectrum of F1-4 showed the same pattern of F2. However, the 1H NMR spectrum of F1-4 showed a difference of only the aromatic part. Comparing them with the 1H peaks of F2, five aromatic proton peaks should be assigned as the benzene ring. From these data, the F1-4 was identified as cyclo(prolylphenylalanyl) (Fig. 2). F1-4 had a molecular formula of $C_{14}H_{16}N_2O_2$ as determined



F2 : R = OH
F1-4 : R = H

Fig. 2. The structures and numbering of F2 and F1-4.

from mass spectrometry, which gave a molecular ion peak at m/z 244. The complete assignments of the ^1H and ^{13}C chemical shifts of cyclo(propylphenylalanyl) are listed in Table 1.

Akt inhibitory effects of F2 and F1-4 were tested using Western blot analysis in U-87MG human glioma cells, as described above. A calmodulin antagonist, clozapine (CZP), was used as a positive control for the inhibition of Akt [10]. Treatment with F2 resulted in 18% reduction, whereas F1-4 resulted in only 3% inhibition in Akt phosphorylation (Fig. 3). By contrast, there was no change in the amounts of GAPDH (bottom panel), demonstrating a true decrease in the Akt phosphorylation level.

Even though the two compounds isolated from *Shrimpeotkal* in our study belong to cyclic dipeptides, their inhibitory effects against Akt are different from each other. In order to elucidate the reasons for these differences, three-dimensional (3D) structural studies were carried out. There are three theoretical methods to obtain the 3D

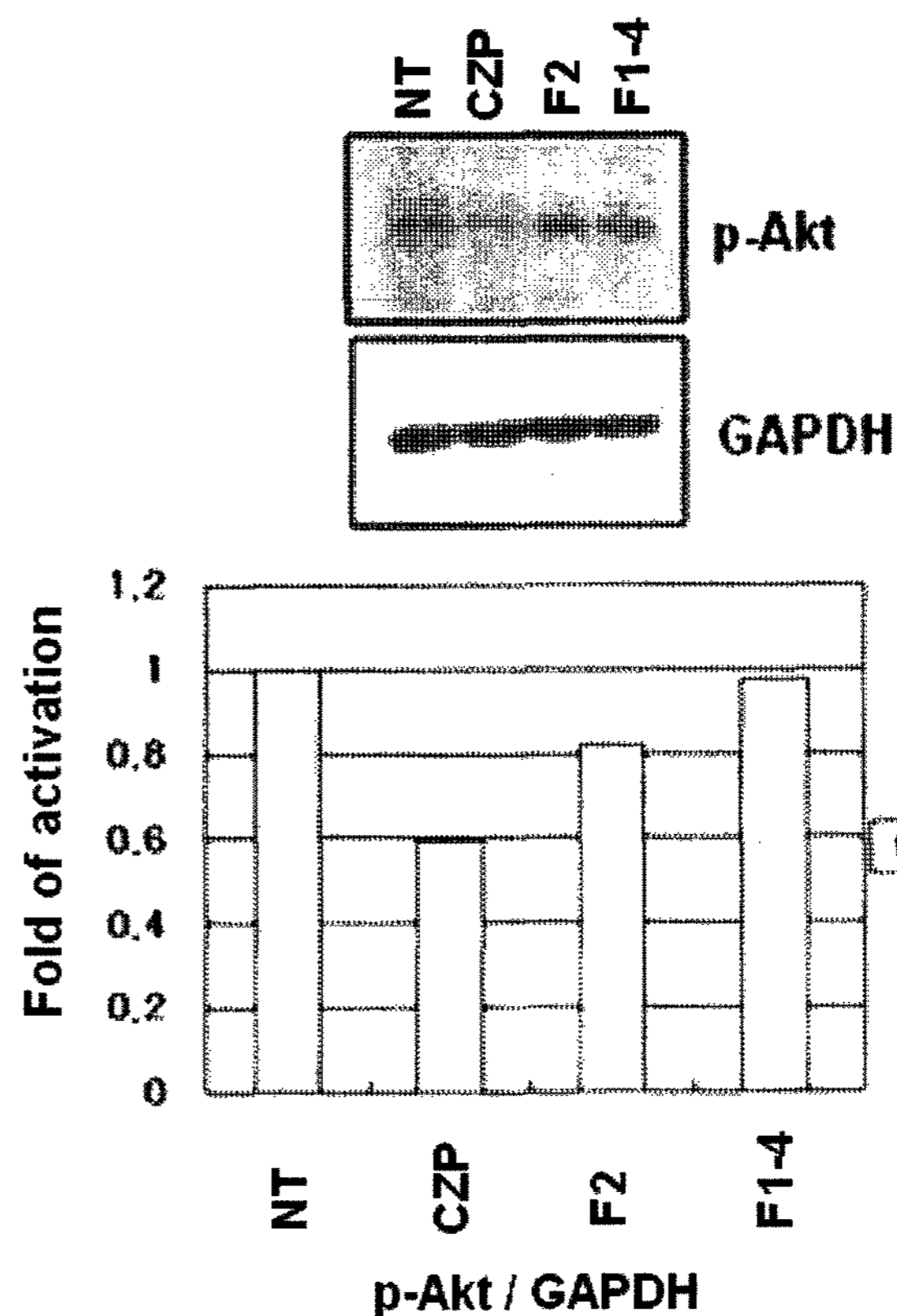


Fig. 3. Akt inhibitory effects of F2 and F1-4 (NT, Not treated; CPZ, clozapine; GAPDH, Glyceraldehydes-3-phosphate dehydrogenase). The densitometric values in densitometry are plotted as mean \pm SD ($n=3$). The statistical significance of the assay was evaluated using Student's t -test ($p<0.05$ compared with not treated).

structures: *ab initio* method, semiempirical method, and empirical method. In this experiment, the *ab initio* method was adapted using the Gaussian 98 program because cyclic dipeptides are small enough to be calculated by

Table 1. The ^1H and ^{13}C NMR data of F2 and F1-4 in $\text{DMSO}-d_6$.

Position	F2		F1-4	
	^{13}C	^1H δ , m, J (Hz)	^{13}C	^1H δ , m, J (Hz)
1	127.0 s		137.2 s	
2,6	130.8 d	7.04 (d, 8.5)	130.0 d	7.25 (m)
3,5	114.7 d	6.63 (d, 8.5)	128.0 d	7.25 (m)
4	155.9 s		126.3 d	7.19 (m)
4-OH		9.23 (bs)		
7	34.7 t	2.92 (dd, 2.8, 4.8)	35.3 t	3.04 (dd, 4.9, 8.0)
8	56.0 d	4.24 (dd, 4.8, 4.8)	55.7 d	4.34 (dd, 4.9, 4.9)
8-NH		7.84 (s)		7.97 (s)
9	165.1 s		165.0 s	
10	58.4 d	4.04 (dd, 7.0, 8.8)	58.4 d	4.07 (dd, 7.0, 8.8)
11	168.9 s		169.0 s	
12	27.8 t	1.40 (m), 1.99 (m)	27.7 t	1.41 (m), 2.00 (m)
13	21.8 t	1.71 (m)	21.9 t	1.72 (m)
14	44.5 t	3.33 (m)	44.6 t	3.33 (m)

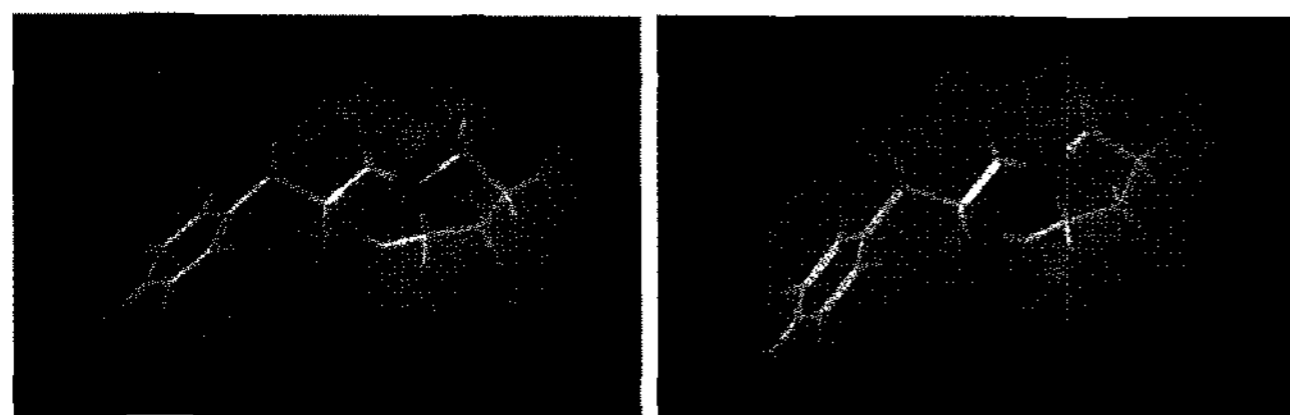


Fig. 4. The three-dimensional structures and Connolly surfaces of F2 (left) and F1-4 (right), obtained from *ab initio* calculations. Green color denotes hydrophilicity and brown color, denotes hydrophobicity.

the *ab initio* method [7, 12]. In addition, another approach is a hybrid density functional method, which includes the Becke's three-parameter functional with the 6-31G basis set incorporated in the Gaussian 98 (Gaussian Com., Wallingford, CT, U.S.A.) used for geometry optimization of the compounds [9]. In the 3D structure of F2 obtained from this calculation, the angles of C9-C8-N, N-C10-C11, N-C14-C13, C10-C12-C13, C9-N-C14, and C11-C10-C12 were 109.025°, 110.042°, 99.579°, 102.855°, 121.420°, and 115.525°, respectively. In that of F1-4, they were 109.034°, 110.050°, 99.586°, 102.869°, 121.421°, and 115.586°, respectively. Furthermore, their 3D structures are shown in Fig. 4 as Connolly surfaces. Because the geometry of F2 obtained from *ab initio* calculations is the same as that of F1-4, their different inhibitory effects cannot be explained. However, from the structures drawn by Connolly surfaces, it is evident that a little hydrophobic difference exists between two compounds. The C-4 position of F2 is more hydrophilic than that of F1-4. The surface, except for C-4 of F2, is the same as that of F1-4.

In conclusion, two cyclic dipeptides isolated from the strain BA34 show different Akt inhibitory effects because they have different hydrophobicities.

Acknowledgments

This work was supported by a grant from Biogreen 21 (Korea Ministry of Agriculture and Forestry) and by a grant from the second Brain Korea 21 (Korea Ministry of Education). Sungwon Hong and Byoung-Ho Moon contributed equally to this work.

REFERENCES

1. Datta, S. R., A. Brunet, and M. E. Greenberg. 1999. Cellular survival: A play in three Akts. *Genes Dev.* **13**: 2905–2927.
2. Downward, J. 1998. Mechanisms and consequences of activation of protein kinase B/Akt. *Curr. Opin. Cell Biol.* **10**: 262–267.
3. Kim, C. G., B. H. Choi, S. W. Son, S. J. Yi, S. Y. Shin, and Y. H. Lee. 2007. Tamoxifen-induced activation of p21^{Waf1/Cip1} gene transcription is mediated by Early Growth Response-1 protein through the JNK and p38 MAP kinase/Elk-1 cascades in MDA-MB-361 breast carcinoma cells. *Cell. Signal.* **19**: 1290–1300.
4. Kim, H. S., Y. S. Yi, G. J. Choi, K. Y. Cho, and Y. Lim. 2006. Antifungal activity of *Bacillus* sp. against *Phytophthora infestans*. *J. Microbiol. Biotechnol.* **16**: 487–490.
5. Lee, C. H., M. W. Kim, H. S. Kim, J. H. Ahn, Y. S. Yi, K. R. Kang, Y. D. Yoon, G. J. Choi, K. Y. Cho, and Y. Lim. 2006. An antifungal property of *Burkholderia ambifaria* against phytopathogenic fungi. *J. Microbiol. Biotechnol.* **16**: 465–468.
6. Lim, H. Y., Y. Lim, Y. H. Cho, and C. H. Lee. 2006. Induction of apoptosis in the HepG2 cells by HY53, a novel natural compound isolated from *Bauhinia forficata*. *J. Microbiol. Biotechnol.* **16**: 1262–1268.
7. Malek, K., V. Martin, H. Kozłowski, and L. M. Proniewicz. 2004. Experimental and theoretical NMR study of selected oxocarboxylic acid oximes. *Magn. Reson. Chem.* **42**: 23–29.
8. Redaelli, C., F. Granucci, L. De Gioia, and L. Cipolla. 2006. Synthesis and biological activity of Akt/PI3K inhibitors. *Mini Rev. Med. Chem.* **6**: 1127–1136.
9. Schaltehaar, G. and J. H. Noordik. 2000. Molden: A pre- and post-processing program for molecular and electronic structures. *J. Comput. Aided Mol. Des.* **14**: 123–134.
10. Shin, S. Y., B. H. Choi, J. Ko, S. H. Kim, Y. S. Kim, and Y. H. Lee. 2006. Clozapine, a neuroleptic agent, inhibits Akt by counteracting Ca²⁺/calmodulin in PTEN-negative U-87MG human glioblastoma cells. *Cell. Signal.* **18**: 1876–1886.
11. Sun, M., G. Wang, J. E. Paciga, R. I. Feldman, Z. Q. Yuan, X. L. Ma, S. A. Shelley, R. Jove, P. N. Tsichlis, S. V. Nicosia, and J. Q. Cheng. 2001. AKT1/PKBalpha kinase is frequently elevated in human cancers and its constitutive activation is required for oncogenic transformation in NIH3T3 cells. *Am. J. Pathol.* **159**: 431–437.
12. Tripathi, A. N., L. Chauhan, P. P. Thankachan, and Ritu Barthwal. 2007. Quantum chemical and nuclear magnetic resonance spectral studies on molecular properties and electronic structure of berberine and berberrubine. *Magn. Reson. Chem.* **45**: 647–655.